



## Tribological analysis of wire additive manufactured Ti-6Al-4V by electron beam source

Manjunath A, Anandakrishnan V <sup>1\*</sup>, Ramachandra S <sup>2</sup>, Parthiban K <sup>2</sup>, Sathish S <sup>3</sup>

<sup>1</sup> Department of Production Engineering, National Institute of Technology Tiruchirappalli, INDIA.

<sup>2</sup> Manufacturing Division, Gas Turbine Research Establishment, INDIA.

<sup>3</sup> Department of Mechatronics Engineering, K.S. Rangasamy College of Technology, INDIA.

\*Corresponding author: krishna@nitt.edu

KEYWORDS	ABSTRACT
Additive manufacturing Wire electron beam Dry sliding wear Wear mechanisms Titanium alloy	Additive manufacturing through electron beam is an attractive and fast-growing additive manufacturing process for complex geometry in the aerospace, automotive and rapid tooling industry. Layer by layer generation of additive material ends up in the variation in properties in each layer gives to a form of functionally graded material. Ti-6Al-4V samples were realized through wire electron beam additive manufacturing by Pre-positioning the wire and then fusing it to the substrate material. Then layer by layer addition was made to realize the bulk additive Ti-6Al-4V material. The samples were subjected to metallurgical analysis to explore structural behaviour and to a standard dry sliding wear test to explore the tribological behaviour. The wear analysis exposed the substantial effects of parameters on the wear rate. The comparison of wear results with the base material under different working conditions shows that the additive manufacture sample has better wear resistance compared with the base alloy. Besides, the mechanisms that significantly influenced the wear rate was identified with worn surface and debris analysis.

Received 20 March 2022; received in revised form 16 June 2022; accepted 8 August 2022.

To cite this article: Anandakrishnan et al. (2023). Tribological analysis of wire additive manufactured Ti-6Al-4V by electron beam source. Jurnal Tribologi 36, pp.86-98.

## 1.0 INTRODUCTION

Material is the heart of engineering and based on its application, it is chosen to meet the product requirements and its functionalities. Based on the property, quantity, features, complexities and economics of the product the suitability of the process of manufacturing material is identified. Though plenty of techniques was there to realize material, the thirst for finding a newer methodology is still not quenched. In that line, additive manufacturing gives an insight with freedom for design and manufacturing with material and energy saving manufacturing (Vayre et al., 2012). Besides the additive manufacturing is versatile in handling the parts with complex geometries (Lizzul et al. 2020). Wire based Electron Beam Additive Manufacturing (EBAM) is an advanced method wherein the wire is fed in line with the beam of electrons, which make the wire melt and gets deposited on the substrate. The electron beam is most suited for the process as it has good control and better penetration with a good rate of deposition, density and bond strength (Kumar and Maji, 2020). Also, the high vacuum of 10-4m bar in the work chamber protects against contamination from the atmosphere (Fuchs et al., 2018). In addition the additive manufacturing through the wire electron beam has the ability to handle large sized components (Kalashnikova et al. 2022). Especially, it is suitable for reactive materials such as titanium alloys which has an extensive range of applications including aircraft components, automotive components and biomedical components owing to its remarkable properties (Cheng et al., 2017; Tan et al., 2011; Palanisamy et al. 2018). Ti-6Al-4V is the material that is widely used in the aerospace industry owing to its good strength-to-weight ratio, higher strength and toughness and admirable corrosion resistance (DiCecco et al., 2021). Although titanium alloys have such excellent properties, their low plastic shear deformation and low work hardening properties make them poor in terms of wear resistance (Wang et al., 2014; Kumar et al. 2019). Though the titanium alloys are made ready in different forms such as cast, wrought, and powder sintered (Matthew J. Donachie, 2000), additive manufacturing is a valued added one that attracts more research attention (Qian and Bourell, 2017). Neikter et al. produced the titanium alloy Ti-6Al-4V through two different additive manufacturing processes (EBM and SLM) and detailed the microstructural characterization of the produced alloy (Neikter et al., 2017). Galarraga et al. made the Ti-6Al-4V alloy through the process of electron beam melting and further heat treated and observed the formation of  $\alpha'$  martensite due to the faster rate of cooling (Galarraga et al., 2017). Yang et al. produced the Ti-6Al-4V alloy through the process of selective laser melting and studied the variations in the formation of  $\alpha$  and  $\beta$  phase with respect to the variation in holding temperatures (Yang et al., 2017). With the electron beam melting technique, different aerospace parts were fabricated with Ti-6Al-4V alloy and found its metallurgical and mechanical properties are equivalent to the bulk materials (Rawal et al., 2013). Though the titanium alloy has excellent properties, the property of wear under friction is very poor and this made an extensive research accomplishment on wear analysis (Pohrelyuk et al., 2016). The wear performance of Ti-6Al-4V alloy was studied under lubricated conditions and observed increased sliding velocity marks in the reduction of wear (Sharma and Sehgal, 2014). The tribological analysis of Ti-6Al-4V alloy was studied under varied load and sliding velocity with dry conditions and observed the wear reduction with increased load and sliding velocity (Kumar et al., 2018). The wear performance of Ti-6Al-4V alloy was studied under a dry sliding state and observed a remarkable transition in the wear mechanisms with respect to sliding velocity (Li et al., 2015). The wear performance of the Ti-6Al-4V alloy was investigated with different parameters and observed a shearing of material with the increased load (Molinari et al., 1997). The wear performance of Ti-6Al-4V alloy sintered through selective laser melting was studied under

lubricated condition and the results showed the occurrence of abrasion, oxidation, and delamination mechanism (Zhu et al., 2016). The literature visibly briefs the earlier attempts of producing titanium Ti-6Al-4V alloy with the additive manufacturing technique and there is no attempt made through the Wire based Electron Beam Additive Manufacturing. It is observed that the Ti-6Al-4V grouped under grade 5 exhibits a poor wear resistance and the alloy has an intended application in the different industries namely aerospace, defence, medical, automobile, marine and sports equipment (Maleque et al., 2018). In particular, bearings of heavy-duty vehicles, disc brakes, rotors and orthopaedics application need many needs an improved wear resistance of titanium alloy (Fellah et al., 2014; Kumar et al., 2018; Philip et al., 2019). The titanium alloy is fabricated through additive manufacturing by prepositioned Ti-6Al-4V wires under different parameters and their influence on the geometry of beads are investigated (Manjunath et al., 2019). The structural parts in automobile and aerospace, sports equipment and medical applications need an improvement in wear resistance and understanding of wear behaviour under sliding conditions. Hence the present research is focused on the development of Ti-6Al-4V alloy through Wire based Electron Beam Additive Manufacturing technique and further investigates its wear characteristics under dry ambient conditions.

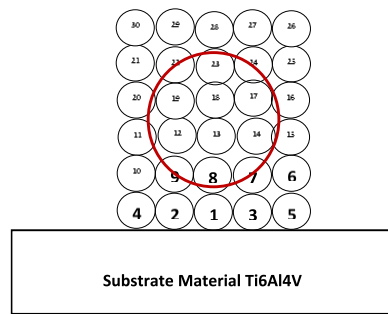
## **2.0 EXPERIMENTAL PROCEDURE**

### **2.1 Wire Additive Manufacturing**

Electron Beam Additive Manufacturing (EBAM) methodology was employed to synthesise the titanium alloy (Ti-6Al-4V) with the pre-positioned wire. The electron beam welding machine of make of Cambridge Vacuum Engineering is used to synthesize the titanium alloy. The titanium alloy filler wire of dimension 2 mm in diameter and the substrate of dimension 100 x 100 x 20 mm is used and its respective chemical composition is shown in Table 1. With resistance welding, the filler wire was pre-positioned over the substrate of the same titanium alloy and the beam of electrons were focused over the prepositioned wire under a vacuum environment of  $2 \times 10^{-4}$  m bar. Thereby the prepositioned wire is melted and gets deposited on the substrate as similar to the process of Direct Metal Deposition process. Three combinations of experiments were attempted by setting 140 kV accelerating voltage, 600 mm/min welding speed and at three variations in beam current (6, 8 and 10 mA). The samples made with the combination of 140 kV accelerating voltage, 600 mm/min welding speed and 8 mA beam current exhibits complete fusion over the substrate, whereas in the other two combinations the fusion is observed at the substrate and noticed a drop through. With the optimal combination and aforesaid procedures, the titanium alloy samples of 7.8 mm width, 7.5 mm height and 100 mm length were made, with 30 successive fusion of prepositioned wire one over the other as required. The wires are preposition in an order of arrangement as shown in Figure 1a and it was deposited through the electron beam source. The typical additive manufactured titanium alloy of through the wire preposition over a length of 100 mm is shown in Figure 1b. The extracted deposited layer was parted for metallurgical analysis and turned to produce the wear test samples of size 6mm diameter and 25mm length. The extracted deposited layer was exposed in the Rigaku Ultima III diffraction machine to obtain the diffraction peaks and Vega 3 Tescan scanning electron microscope to sightsee surface morphology.

Table 1: Chemical composition of titanium alloy.

Material	Al	Va	C	N	O	H	Fe	Y	Ti
Substrate - Ti6Al4V	6.0	4.0	0.10	0.05	0.20	0.012	0.30	-	Balance
Wire - ERTi6Al4V	6.7	4.5	0.05	0.03	0.18	0.015	0.30	0.005	Balance



(a)

(b)

Figure 1: Preposition titanium alloy additive manufacturing (a) schematic sketch (b) build sample.

## 2.2 Wear Experiment

The wear pins obtained through the wire additive manufacturing process were polished at their ends by following the standard procedure. Then the pins underwent the wear experiment in the dry sliding condition as per ASTM G99, in pin-on-disc equipment. The hardened D3 steel is used as the counterpart material for the dry sliding wear test. The merits of performing the experiments in pin-on-disc equipment is a simple and effective technique to evaluate the material wear in a non-abrasive sliding condition. By considering the parameters load, sliding velocity and sliding distance, the wear experiments were conducted for 3000 m sliding distance at varied sets of load (i.e., 9.81, 19.62 and 29.43 N) and sliding velocity (i.e., 1, 2 and 3 m/s) (Alam and Haseeb, 2002; An et al., 2018; Dutt Sharma and Sehgal, 2012; Li et al., 2015; Ming et al., 2006; Revankar et al., 2017; Sathish et al., 2019). Upon the accomplishment of wear experiments, the amount of material worn is identified with the linear wear, which is further transformed to general form wear rate using the expression (1) (Sathish et al., 2019, 2020).

$$Wear\ rate, mm^3m^{-1} = \frac{\frac{\pi}{4} \times (\text{Diameter of pin})^2 \times \text{Linear wear in pin}}{\text{Sliding distance}} \quad (1)$$

## 3.0 RESULTS AND DISCUSSION

### 3.1 Metallurgy of Additive Manufactured Titanium Alloy

To examine and compare the phase existence in the additive manufactured titanium alloy with the base titanium alloy, both the materials were x-ray diffracted and the results were plotted as shown in Figure 2. The diffraction obtained for the base material match with the reference pattern 98-008-0571 exhibits the alpha titanium with (hkl) indices of (002), (011), (012), and (013). The

diffraction obtained for the additive processed material is in the match with the reference pattern 98-009-2053 exhibits the titanium with (hkl) indices of (010), (002), (011), (012), and (013). The observed peak intensities of the additive manufactured sample are found to increase compared to the base material and this is due to the modification of material structure as observed in Figure 2. Figure 3 shows the microstructure of base titanium alloy and additive manufactured titanium alloy. The base titanium alloy exhibits the equiaxed alpha and beta structure and the additive titanium alloy exhibits the needle-shaped acicular  $\alpha$  phase (elongated structure) with the transformation of beta due to rapid cooling of material (Matthew J. Donachie, 2000).

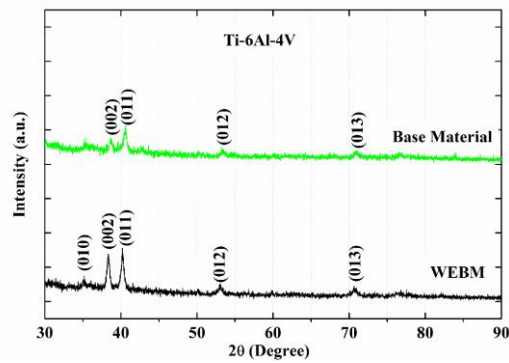


Figure 2: X-ray diffraction of titanium alloy.

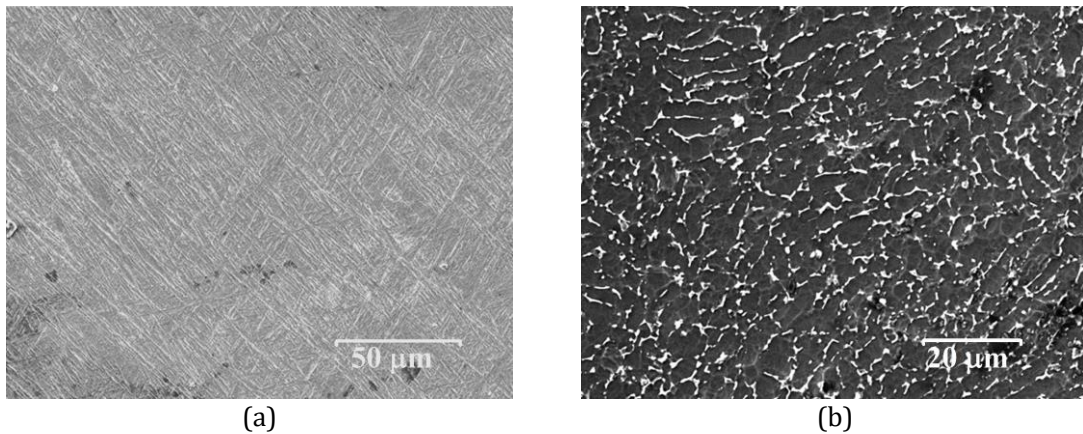


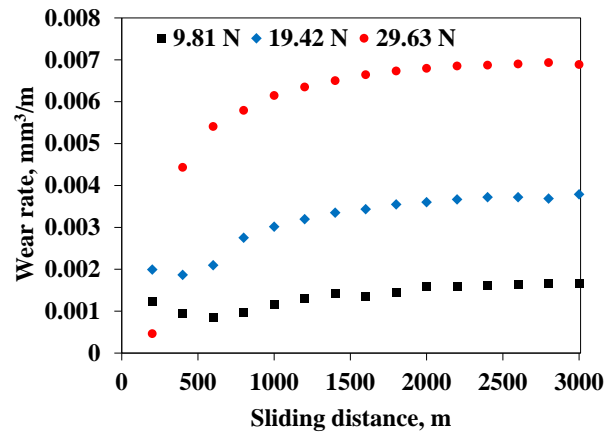
Figure 3: Microstructure of titanium alloy (a) wire additive manufactured (b) base material.

### 3.2 Wear Performance

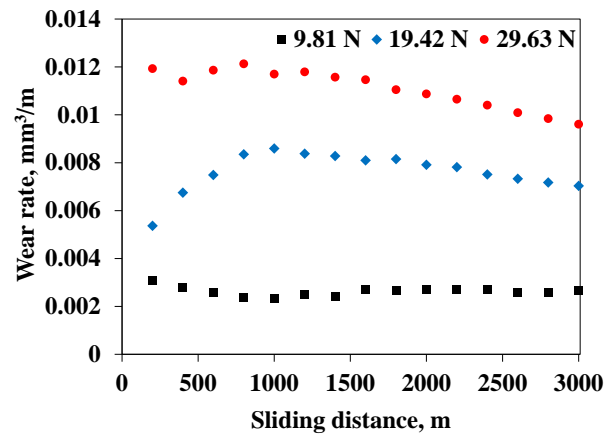
The additive manufactured titanium alloy exposed to dry sliding wear exhibited the wear rate as shown in Figure 4. The exhibited wear rate of titanium alloy under 1 m/s sliding velocity at varied loads are depicted in Figure 4a, the wear rate of additively manufactured titanium alloy shows a lower wear rate at the lower load of 9.81 N and it exhibits a higher wear rate at a higher load of 29.43 N. When the load was at medium level i.e., 19.62 N, it exhibits an intermediate wear rate between the lower and higher condition. The wear rate is found to be in steady-state after 1500 m sliding for the higher and medium loads, whereas at lower load it is achieved after 2500

m sliding distance. This is due to the higher frictional force acting on the sliding surface at higher loads results in the reduction of asperity-to-asperity contact. A similar trend of wear rate was perceived in the additive manufactured titanium under 2 m/s sliding velocity (Figure 4b). But the reduction of wear is visible after the 1500 m sliding distance at medium and higher load, which is resulted from the oxidation mechanism, at increased sliding velocity and load. Whereas at lower load, there is no such declining trend, this shows there is not enough amount of frictional force and temperature to induce the oxidation formation. Though the wear rate of titanium alloy at 3 m/s (Figure 4c) seems to be similar to 1 m/s and 2 m/s, the wear rate at lower and medium load is found to be increased at the initial run and it is declined up to the sliding distance of 1000 m. The possible effect of this reduction is the surface oxidation of the contact asperities at the initial run period due to higher contact stress. Beyond 1000 m sliding distance, it showed an increasing trend of wear rate and it is due to the removal of oxidized asperities from the pin surface. Almost in all the velocities, higher load exhibited higher wear rate and drop in load results in a reduction in wear rate. Initially, the wear rate seems to be lower at the lower sliding velocity and it was found to be increasing with the increase in sliding velocity to 2 m/s. Further, the increase in sliding velocity decreased the wear rate, and this is attributed due to the mechanism of oxidation. A similar trend of reduction in wear rate with an increased sliding velocity and increased wear rate with increased load is reported by Straffelini and Molinari (Straffelini and Molinari, 1999). The comparison of wear results with the base material under different working conditions is presented in Table 2, which shows that the additive manufacture sample has better wear resistance compared with the base alloy.

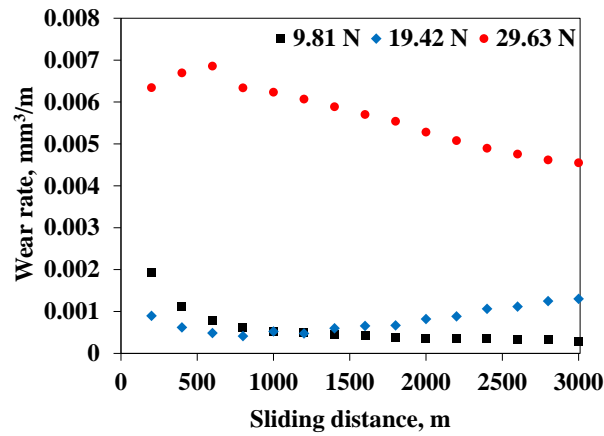
The additive manufactured titanium alloy exposed to dry sliding wear exhibited the coefficient of friction as shown in Figure 5. The exhibited coefficient of friction of the titanium alloy under 1 m/s sliding velocity at varied loads is shown in Figure 5a. It shows a higher coefficient of friction at higher load and it got reduced with the reduction in load. Also, there is a slight fluctuation in the coefficient of friction and this is due to the variation in the surface topography during sliding. A similar trend was observed under the sliding velocity of 3 m/s (Figure 5c), whereas for the sliding velocity of 2 m/s (Figure 5b), the coefficient of friction is higher for medium load for 19.62 N load. The possible reason for this is at sliding velocity 3 m/s, oxidation occurs, which leads to the reduction in coefficient of friction as the oxide layer acts as a lubricant. Also, the coefficient of friction is found to be reduced with the increase in sliding velocity and this effect is due to the formation of the oxide layer.



(a)

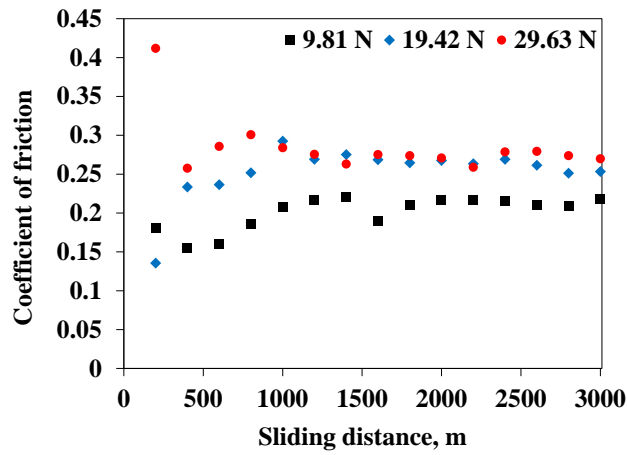


(b)

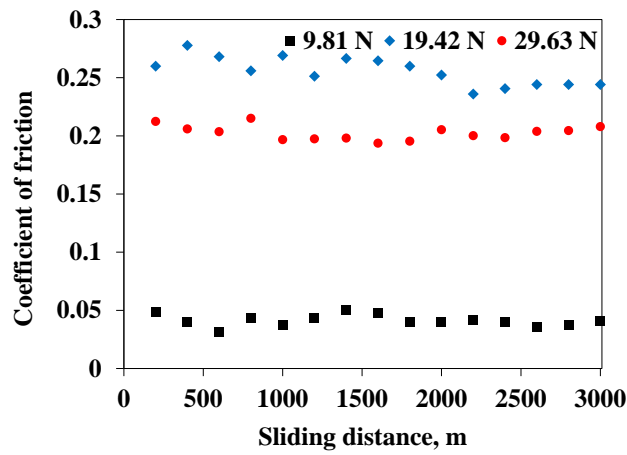


(c)

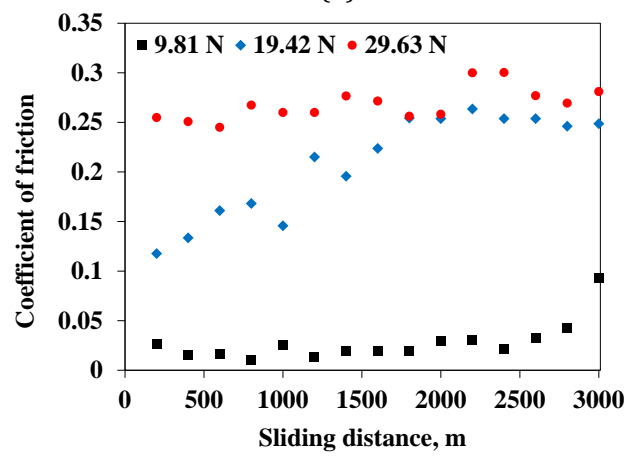
Figure 4: Wear rate of titanium alloy at different sliding velocity (a) 1 m/s (b) 2 m/s (3) 3 m/s.



(a)



(b)



(c)

Figure 5: Coefficient of titanium alloy at different sliding velocity (a) 1 m/s (b) 2 m/s (3) 3 m/s.



Table 2: Comparison of wear rate of titanium alloy.

S. No	Load, N	Sliding Velocity, m/s	Sliding Distance, m	Wear rate mm <sup>3</sup> /m	
				Additive Ti6Al4V	Base Ti6Al4V
1	9.81	1	3000	0.001670	0.001739
2	9.81	2	3000	0.002664	0.002035
3	9.81	3	3000	0.000164	0.000932
4	19.62	1	3000	0.003789	0.003875
5	19.62	2	3000	0.007035	0.004834
6	19.62	3	3000	0.000627	0.002835
7	29.43	1	3000	0.006887	0.007052
8	29.43	2	3000	0.009608	0.010128
9	29.43	3	3000	0.004550	0.003655

### 3.3 Wear Mechanism

The dry sliding of the titanium alloy pin results in the destruction of the sliding surface, which helps to reveal the involved wear mechanism. After dry sliding, the pin which exhibits the best wear rate and worst wear rate was analysed under a scanning electron microscope as shown in Figure 6. The surface topography of the wear pin corresponds to the worst wear (i.e., the load of 29.43 N with the sliding velocity of 2 m/s) in Figure 6a, it shows the presence of crater, scratches, and spalling that evident in the delamination, and abrasion mechanism. The observation of fragments and laminates confirms the mechanism of delamination and abrasion from Figure 6a. The topography of the wear pin surface corresponds to the best wear (i.e., the load of 9.81 N with the sliding velocity of 3 m/s) is shown in Figure 6b, with spalling, ridges, shallow crater, ploughs, and scratches. The ridges on observed surface morphology raised due to the deformation of deformed layers due to adhesion and the ploughs and scratch evident abrasion mechanism. The observation of ribbon flakes confirms the abrasion mechanism, laminates confirm the delamination mechanism and fine debris confirms the mechanism of oxidation from Figure 7a and 7b. The mechanism of oxidation is confirmed with the presence of oxygen content in the worn pin corresponds to the best wear condition.

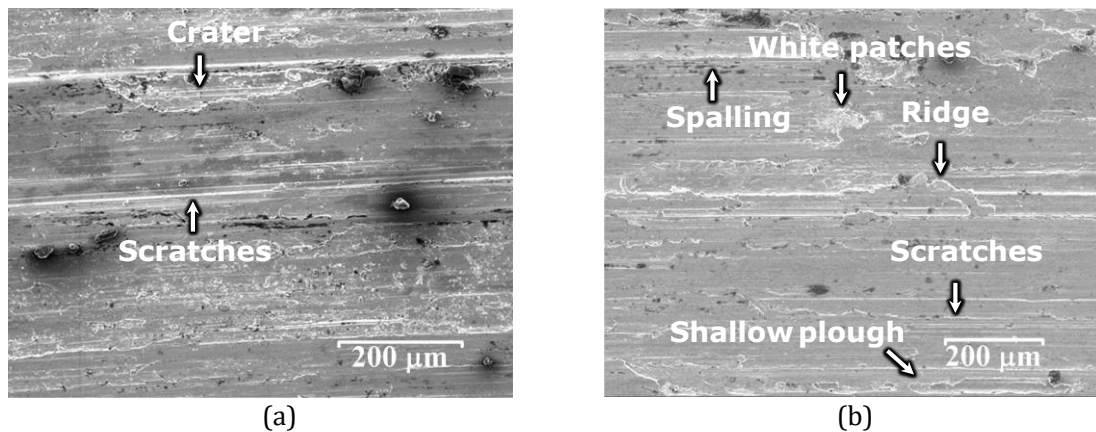


Figure 6: Worn surface of additive manufactured titanium alloy (a) worst condition (b) best condition.

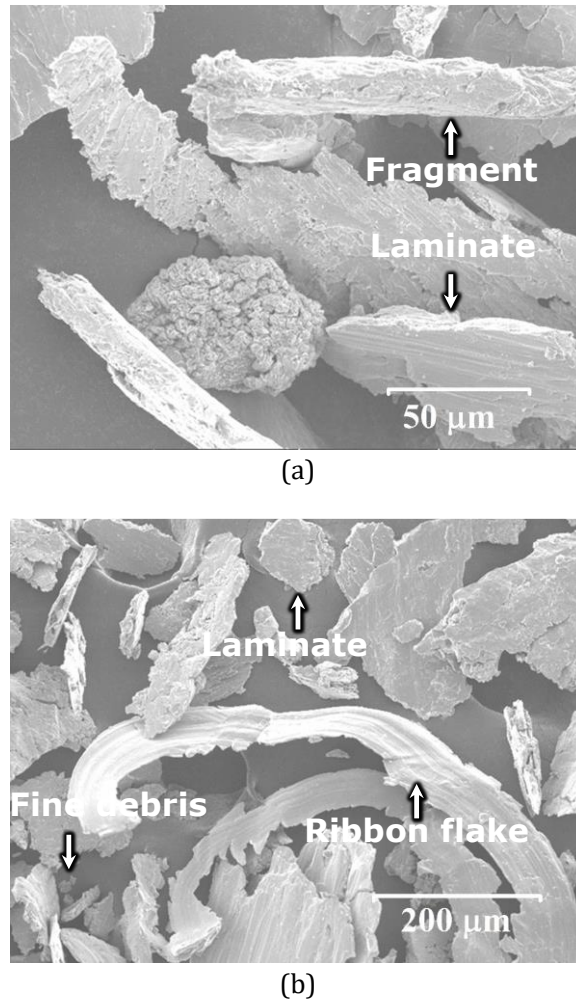


Figure 7: Debris analysis of additive manufactured titanium alloy (a) worst condition (b) best condition.

## CONCLUSION

Ti-6Al-4V alloy was produced through additive manufacturing using Electron Beam with pre-positioned wire and its metallurgy was analysed. The additive manufactured titanium alloy exhibits a needle-shaped acicular  $\alpha$  phase due to the rapid cooling. The wear analysis showed the increased rate of wear with an increased load and the increased sliding velocity exhibits a reduction in wear rate. Also, it was noticed that the rate of wear is increased initially and then it reduced at medium sliding velocity with high and medium loads. The investigation on the worn surface under the microscopic level exhibit the surface topographies with crater, ploughs, scratches, white patches and spalling, manifest the delamination, adhesion, oxidation and abrasion mechanism. Similarly, the collected debris exhibit the laminates, ribbon fragments, and fine debris confirms the above delamination, adhesion, oxidation and abrasion mechanism.

## REFERENCES

- Alam, M. O., & Haseeb, A. S. M. A. (2002). Response of Ti-6Al-4V and Ti-24Al-11Nb alloys to dry sliding wear against hardened steel. *Tribology International*, 35(6), 357–362. doi: 10.1016/S0301-679X(02)00015-4
- An, Q., Huang, L. J., Bao, Y., Zhang, R., Jiang, S., Geng, L., & Xiao, M. (2018). Dry sliding wear characteristics of in-situ TiBw/Ti6Al4V composites with different network parameters. *Tribology International*, 121(October 2017), 252–259. doi: 10.1016/j.triboint.2018.01.053
- Cheng, C., Dou, Z. H., Zhang, T. A., Zhang, H. J., Yi, X., & Su, J. M. (2017). Synthesis of As-Cast Ti-Al-V Alloy from Titanium-Rich Material by Thermite Reduction. *Jom*, 69(10), 1818–1823. doi: 10.1007/s11837-017-2467-7
- DiCecco, L. A., Mehdi, M., & Edrisy, A. (2021). Dry-Sliding Wear Mechanisms of Shot-Peened Additive Manufactured Alpha Titanium Featuring TiB Particles. *Tribology Letters*, 69(3), 1–15. doi: 10.1007/s11249-021-01456-4
- Dutt Sharma, M., & Sehgal, R. (2012). Dry Sliding Friction and Wear Behaviour of Titanium Alloy (Ti-6Al-4V). *Tribology Online*, 7(2), 87–95. doi: 10.2474/trol.7.87
- Fellah, M., Laba, M., Assala, O., Dekhil, L., Taleb, A., Rezag, H., & Iost, A. (2014). Tribological behavior of Ti-6Al-4V and Ti-6Al-7Nb Alloys for Total Hip Prosthesis. *Advances in Tribology*, 2014, 13. doi: https://doi.org/10.1155/2014/451387.
- Fuchs, J., Schneider, C. & Enzinger, N. (2018). Wire-based additive manufacturing using an electron beam as heat source. *Welding in the World*, 62(2), 267–275. Doi: https://doi.org/10.1007/s40194-017-0537-7
- Galarraga, H., Warren, R. J., Lados, D. A., Dehoff, R. R., Kirka, M. M., & Nandwana, P. (2017). Effects of heat treatments on microstructure and properties of Ti-6Al-4V ELI alloy fabricated by electron beam melting (EBM). *Materials Science and Engineering A*, 685(February), 417–428. doi: 10.1016/j.msea.2017.01.019
- Kalashnikova, T., Chumaevskii, A., Kalashnikov, K., Knyazhev, E., Gurianov, D., Panfilov, A., Nikonov, S., et al. (2022). Regularities of Friction Stir Processing Hardening of Aluminum Alloy Products Made by Wire-Feed Electron Beam Additive Manufacturing. *Metals*, 12(2). https://doi.org/10.3390/met12020183.
- Kumar, A., & Maji, K. (2020). Selection of Process Parameters for Near-Net Shape Deposition in Wire Arc Additive Manufacturing by Genetic Algorithm. *Journal of Materials Engineering and Performance*, 29(5), 3334–3352. doi: 10.1007/s11665-020-04847-1
- Kumar, D., Deepak, K. B., Muzakkir, S. M., Wani, M. F., & Lijesh, K. P. (2018). Enhancing tribological performance of Ti-6Al-4V by sliding process. *Tribology - Materials, Surfaces and Interfaces*, 12(3), 137–143. doi: 10.1080/17515831.2018.1482676
- Kumar, D., Lal, B., Wani, M.F., Philip, J.T. & Kuriachen, B. (2019). Dry sliding wear behaviour of Ti-6Al-4V pin against SS316L disc in vacuum condition at high temperature. *Tribology - Materials, Surfaces and Interfaces*, 13 (3), 182–189. Doi: 10.1080/17515831.2019.1637148
- Li, X. X., Zhou, Y., Ji, X. L., Li, Y. X., & Wang, S. Q. (2015). Effects of sliding velocity on tribo-oxides and wear behavior of Ti-6Al-4V alloy. *Tribology International*, 91, 228–234. doi: 10.1016/j.triboint.2015.02.009
- Lizzul, L., Sorgato, M., Bertolini, R., Ghiotti, A. & Bruschi, S. (2020). Influence of additive manufacturing-induced anisotropy on tool wear in end milling of Ti6Al4V. *Tribology International*, 146, 106200. https://doi.org/10.1016/j.triboint.2020.106200
- Maleque, A., Harina, L., Bello, K., Azwan, M., & Rahman, M. (2018). Tribological properties of surface modified Ti-6Al-4V alloy under lubricated condition using Taguchi approach. *Jurnal*

- Tribologi*, 17, 15–28.
- Manjunath, A., Anandakrishnan, V., Ramachandra, S., & Parthiban, K. (2019). Experimental investigations on the effect of pre-positioned wire electron beam additive manufacturing process parameters on the layer geometry of titanium 6Al4V. *Materials Today: Proceedings*, 21(1), 766–772. doi: 10.1016/j.matpr.2019.06.727
- Matthew J. Donachie, J. (2000). Titanium - A Technical Guide. In *ASM International*. doi: 10.5772/1844
- Ming, Q., Yong-zhen, Z., Jian-heng, Y., & Jun, Z. (2006). Microstructure and tribological characteristics of Ti-6Al-4V alloy against GCr15 under high speed and dry sliding. *Materials Science and Engineering A*, 434(1–2), 71–75. doi: 10.1016/j.msea.2006.07.043
- Molinari, A., Straffelini, G., Tesi, B., & Bacci, T. (1997). Dry sliding wear mechanisms of the Ti6Al4V alloy. *Wear*, 208(1–2), 105–112. doi: 10.1016/S0043-1648(96)07454-6
- Neikter, M., Åkerfeldt, P., Pederson, R., & Antti, M. L. (2017). Microstructure characterisation of Ti-6Al-4V from different additive manufacturing processes. *IOP Conference Series: Materials Science and Engineering*, 258(1). doi: 10.1088/1757-899X/258/1/012007
- Palanisamy, C., Bhero, S., Abiodun Obadele, B. & Apata Olubambi, P. (2018). Effect of build direction on the microhardness and dry sliding wear behaviour of laser additive manufactured Ti-6Al-4V. *Materials Today: Proceedings*, 5(1), 397–402. <https://doi.org/10.1016/j.matpr.2017.11.097>
- Philip, J. T., Mathew, J., & Kuriachen, B. (2019). Tribology of Ti6Al4V : A review. *Friction*, 7(6), 497–536.
- Pohrellyuk, I. M., Tkachuk, O. V., Proskurnyak, R. V., Boiko, N. M., Kluchivska, O. Y., & Stoika, R. S. (2016). Effect of Thermodiffusion Nitriding on Cytocompatibility of Ti-6Al-4V Titanium Alloy. *Jom*, 68(4), 1109–1115. doi: 10.1007/s11837-016-1824-2
- Qian, M., & Bourell, D. L. (2017). Additive Manufacturing of Titanium Alloys. *Jom*, 69(12), 2677–2678. doi: 10.1007/s11837-017-2630-1
- Rawal, S., Brantley, J., & Karabudak, N. (2013). Additive manufacturing of Ti-6Al-4V alloy components for spacecraft applications. *RAST 2013 - Proceedings of 6th International Conference on Recent Advances in Space Technologies*, 5–11. doi: 10.1109/RAST.2013.6581260
- Revankar, G. D., Shetty, R., Rao, S. S., & Gaitonde, V. N. (2017). Wear resistance enhancement of titanium alloy (Ti-6Al-4V) by ball burnishing process. *Journal of Materials Research and Technology*, 6(1), 13–32. doi: 10.1016/j.jmrt.2016.03.007
- Sathish, S., Anandakrishnan, V., & Gupta, M. (2020). Optimization of tribological behavior of magnesium metal-metal composite using pattern search and simulated annealing techniques. *Materials Today: Proceedings*, 21, 492–496. doi: 10.1016/j.matpr.2019.06.643
- Sathish, S., Anandakrishnan, V., & Manoj, G. (2019). Optimization of wear parameters of Mg-(5.6 Ti+ 3Al)-2.5 B4C composite. *Industrial Lubrication and Tribology*, 72(4), 503–508. doi: 10.1108/ILT-08-2019-0326
- Sathish, S., Anandakrishnan, V., Sankaranarayanan, S., & Gupta, M. (2019). Optimization of wear parameters of magnesium metal-metal composite using Taguchi and GA technique. *Jurnal Tribologi*, 23, 76–89.
- Sharma, M. D., & Sehgal, R. (2014). Experimental study of friction and wear characteristics of titanium alloy (Ti-6Al-4V) under lubricated sliding condition. *Industrial Lubrication and Tribology*, 66(2), 174–183. doi: 10.1108/ILT-10-2011-0079
- Straffelini, G., & Molinari, A. (1999). Dry sliding wear of Ti-6Al-4V alloy as influenced by the counterface and sliding conditions. *Wear*, 236(1–2), 328–338. doi: 10.1016/S0043-

1648(99)00292-6

- Tan, W., Stoschka, M., Riedler, M., Eichlseder, W., Romagnoli, F., & Rondon, V. (2011). Material and component investigations on a Ti-6-4 fitting element. *Mechanics & Industry*, 12(5), 361–378. doi: 10.1051/meca/2011130
- Vayre, B., Vignat, F., & Villeneuve, F. (2012). Metallic additive manufacturing: state-of-the-art review and prospects. *Mechanics & Industry*, 13(2), 89–96. doi: 10.1051/meca/2012003
- Wang, L., Zhang, Q. Y., Li, X. X., Cui, X. H., & Wang, S. Q. (2014). Severe-to-mild wear transition of titanium alloys as a function of temperature. *Tribology Letters*, 53(3), 511–520. doi: 10.1007/s11249-013-0289-5
- Yang, Y., Liu, Y. J., Chen, J., Wang, H. L., Zhang, Z. Q., Lu, Y. J., ... Lin, J. X. (2017). Crystallographic features of  $\alpha$  variants and  $\beta$  phase for Ti-6Al-4V alloy fabricated by selective laser melting. *Materials Science and Engineering A*, 707(July), 548–558. doi: 10.1016/j.msea.2017.09.068
- Zhu, Y., Chen, X., Zou, J., & Yang, H. (2016). Sliding wear of selective laser melting processed Ti6Al4V under boundary lubrication conditions. *Wear*, 368–369, 485–495. doi: 10.1016/j.wear.2016.09.020